Osteoarthritis and Cartilage Open 7 (2025) 100557

Contents lists available at ScienceDirect

Osteoarthritis and Cartilage Open

journal homepage: www.elsevier.com/journals/osteoarthritis-and-cartilage-open/2665-9131

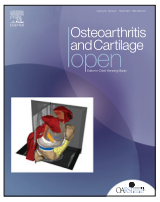

CT scan-based morphometric comparison of human and canine lumbar spine generates instrumental data for intervertebral disc percutaneous surgery

N. Gavira [a,f], C. Decante [a,f], N. Bouhsina [a], D. Rouleau [a], B. Miannay [b], N. Bronsard [c], A. David [d], R. Jossier [e], O. Gauthier [a], A. Hamel [a], J. Guicheux [a], J. Clouet [a,g], M. Fusellier [a,*,g]

[a] Nantes Université, Oniris, CHU Nantes, INSERM, Regenerative Medicine and Skeleton, RMeS, UMR 1229, Nantes, F-44000, France
[b] Data-Prisme La Réunion, France[h]
[c] CHU Nice, Service orthopédie et traumatologie, France
[d] CHU Nantes, Service d'imagerie médicale, PHU6, Nantes, F-44093, France
[e] Clinique VetRef, Beaucouzé, 49070, France

ARTICLE INFO

Handling Editor: Professor H Madry

Keywords:
Intervertebral disc
Human and animal model
Transpedicular and transannular approach
Regenerative medicine
Canine model

ABSTRACT

Objective: This study aimed to describe the anatomical landmarks for intervertebral disc (IVD) percutaneous approaches (transpedicular TPA and transannular TAA) using CT scans in humans and dogs for regenerative medicine research.
Method: CT scans of 57 human (30 supine, 27 prone) and 49 canine (29 chondrodystrophic, 20 non-chondrodystrophic) lumbar spines were analyzed. Morphometric data, cutaneous landmarks, and approach angles were measured, with additional sections assessing nerve root distances from TPA routes.
Results: Over 15,000 measurements were taken, creating a comprehensive anatomical database. Significant differences in TPA and TAA angles were noted between humans and dogs ($p < 0.0001$).
Conclusion: This study provides detailed anatomical landmarks for safe and effective IVD approaches, offering valuable guidance for translational research and surgical interventions.

1. Introduction

Degenerative intervertebral disc disease (DDD) is responsible for approximately 40 % of low back pain (LBP) [1]. Because of its socio-economic impact related to treatments and loss of productive time [2], recent studies have focused on improving our understanding of the pathogenic mechanisms leading to intervertebral disc (IVD) spontaneous degeneration and of regenerative ways of treatment [3]. Researchers have been working on innovative therapeutic product injection (biomaterial, regenerative cells sources, biological factors …) to regenerate the N*ucleus pulposus* (NP) [4]. The approach's choice to safely inject into the NP is crucial. Currently, the percutaneous dorsolateral route under fluoroscopic control, namely transannular approach (TAA), is considered as reference for reaching the NP by needle puncture of the *annulus fibrosus* (AF) [5]. Regarding the potential risk of accelerated IVD degeneration post-injection through the AF, new approaches have been investigated, notably the *trans*-pedicular approach (TPA) [6,7] Briefly, TPA consists in reaching the NP, without AF lesion, through the caudal vertebra by successively crossing the pedicle, the vertebral body, and the endplate.

In this context, validation of the feasibility on the NP routes on animal models in order to guarantee safety is necessary before applying them to

This article is part of a special issue entitled: Joint Regeneration published in Osteoarthritis and Cartilage Open.

* Corresponding author. Department of Diagnostic Imaging, ONIRIS, College of Veterinary Medicine, Food Science and Engineering, Nantes, F-44307, France.
E-mail addresses: nathaly.gavira@gmail.com (N. Gavira), cyrille.decante@chu-nantes.fr (C. Decante), nora.bouhsina@oniris-nantes.fr (N. Bouhsina), dominique.rouleau@oniris-nantes.fr (D. Rouleau), bertrandmiannay@gmail.com (B. Miannay), bronsard.n@chu-nice.fr (N. Bronsard), arthur.david@chu-nantes.fr (A. David), dr.jossier@gmail.com (R. Jossier), olivier.gauthier@oniris-nantes.fr (O. Gauthier), antoine.hamel@chu-nantes.fr (A. Hamel), jerome.guicheux@univ-nantes.fr (J. Guicheux), johann.clouet@univ-nantes.fr (J. Clouet), marion.fusellier@oniris-nantes.fr (M. Fusellier).
[f] Co-first authors.
[g] Co-last authors.
[h] https://www.data-prisme.com/.

https://doi.org/10.1016/j.ocarto.2024.100557
Received 19 February 2024; Accepted 5 December 2024

humans. Beyond the technical approach, the choice of animal model is essential [8]. Animal models should mimic the human vertebral anatomy and, if possible, present a similar IVD degeneration. The canine model is less frequently used because of ethical questioning and its great heterogeneity. Nevertheless, among the breeds, chondrodystrophic dogs exhibit spontaneous early DDD and thus could constitute a relevant model in the context of the development of clinical tests in IVD regenerative medicine [9–11]. Thus, canine patients could serve as an excellent preclinical model for studying disc disease and regenerative therapeutic pathways. Moreover, disc degeneration is highly prevalent in dogs, particularly in chondrodystrophic breeds, leading to a significant risk of disc herniation. The canine patient population could greatly benefit from the new treatments being developed.

Therefore, knowledges about lumbar anatomy in canine and human models is particularly relevant to anticipate potential limitations to a future human transposition. The study of the spine in both humans and dogs has long benefited from the superiority of Computed tomography scan (CT-scan) over 2D radiography. Indeed, CT scanning allows for 3D evaluation of bone structures, enabling the measurement of angles that cannot be assessed on sagittal and frontal planes obtained by X-ray. Moreover, it is currently the most widely used technique for detecting IVD disorders in both species. Currently, CT-scans are primarily used for diagnostic purposes and rarely serve as a basis for angle measurements, as surgical landmarks are relatively consistent from one patient to another. In dogs, since intradiscal injections are rare, these angle measurements hold little significance. However, as dogs are increasingly being used as preclinical models for regenerative disc therapy and are even becoming targets for treatments, it is essential for surgeons to have anatomical landmarks that allow for safe approaches to the IVD. Thus, the aims of this study were to describe the precise anatomical landmarks required for a safe IVD percutaneous approaches in human and canine models, both chondrodystrophic and non-chondrodystrophic, using CT-scan.

2. Methods

2.1. Population and group distribution

The human group (H) gathers 57 CT-scans. This group had a total of 285 vertebrae and 342 IVD and was divided into 2 groups. The first group contained 30 Supine Position Human (SPH) CT-scans (Light Speed®, GE Medical Systems VCT, Nice, France, helicoidal, slice thickness 0.625–1.25 mm, 120 kV, 147–451 mA). Gender repartition was 11 women (36.7 %) and 19 men (63.6 %). Mean age was 60.7 years (35–87 years). SPH are abdominal CT-scans from the "Lombonice 2005" database. The second group contained 27 Prone Position Human (PPH) CT-scans from Nantes' database (Somaton ®, Definition AS, Siemens, Nantes, France helicoidal, slice thickness 1.5–4 mm, 100–140 kV, 385–657 mA). Gender repartition in PPH group was 10 women (37 %) and 17 men (63 %) Mean age was 67.3 years (25–90 years) and mean weight was 75 kg ± 18.5. PPH CT-scans were performed during interventional procedures.

The canine group consists in 49 CT-scans (343 vertebrae and 392 IVD) from dogs consulting the veterinary clinic VetRef (Angers) and that underwent a CT-scan under general anesthesia for reasons other than spinal examination. Animals in which vertebral lesions were detected were excluded. The first group noted LG for Labrador and Golden retriever, contained 20 prone position CT-scans from non-chondrodystrophic medium sized dogs. There were 18 Labrador and 2 Golden retrievers. Mean age was 6.5 years (1–13 years). The group has 10 females (50 %) and 10 males (50 %). The second group, noted FB for French bulldog, contained 29 prone position CT-scans from chondrodystrophic dogs under general anesthesia. Mean age was 4.8 years (2–9 years). They were 8 females (27.6 %) and 21 males (72.4 %). All CT-scan were performed under general anesthesia (Aquilion®, Toshiba, Vetref, Angers, France, helicoidal, slice thickness 1–2 mm, 120 kV, 200 mA).

2.2. Anatomical measurements

CT-scan measurements from all the bony anatomical vertebral reliefs and IVDs have been performed as shown in Fig. 1. The image data were analyzed and measurements were performed by a single investigator, orthopedic surgeon trained in interpreting spinal CT scans in her daily practice (Horos software 3.0®) (Fig. 1). These measurements are of clinical interest for surgical approaches and the evaluation of disc degeneration, particularly IVD cranio-caudal distance (O) allows the evaluation of DDD, spinous process ventro-dorsal distance (P) and the angles for the surgical approaches. The other measurements are mainly used for comparative anatomy purposes.

2.3. Landmarks measurements

Concerning the TPA, 3 angles were measured to describe the path, since it involves the 3 planes of space (ascending path passing through the pedicle and reaching the Nucleus pulposus). Indeed, the transpedicular approach requires drilling into the pedicles to create access to the intervertebral disc through the vertebral body without damaging the *Annulus fibrosus* while avoiding injury to adjacent neural structures. To achieve this, it is necessary to measure three angles (a), (b), and (c), which are measured respectively in the sagittal, transverse, and frontal planes to determine the angulation of the surgical instruments from the skin incision to the center of the disc (Fig. 2).

Concerning the TAA, all measurements were performed on images obtained in a strictly transverse plane and summarized in Fig. 3 aTAA angle was the mean between minimal angle (l) and maximal angle (m). Minimal (n) and maximal (o) distances between the medial line and the cutaneous entry point for (l) and (m) were measured avoiding spinal canal and abdominal compartment. Finally, distances between the cutaneous entry for (l) and (m) angles and NP were measured. They were noted (p) and (q) respectively.

2.4. Lumbar spine anatomical sagittal sections of a human and a dog in a plane of TPA routes

To analyze the distances between the nerve roots and the TPA routes, an additional dog was used. 4 TPA were performed *ex vivo* with a Kirschner wire under radioscopy using angles previously established. The spine was then removed, frozen and sections were performed in the plane of the wires. For Human, a section in the theoretical sagittal plan of the TPA was made by a virtual dissection table (Anatomage® Table 7.0 – Milan). The distances between the Kirschner wires and the adjacent nerve roots were measured.

2.5. Statistical analysis

The statistical analysis was performed with R software. The intra-rater reliability was assessed using a linear mixed-effects model and considered to be excellent if the value of the intraclass correlation coefficient (ICC) was greater than 0.90. The same vertebra was measured 15 times at 24 h interval by the same investigator. Mean values and standard deviations were calculated with Excel (Microsoft 2004).

Concerning morphometric data, no statistic test was performed to avoid irrelevant comparison, the results provided are the average data obtained in each model. These data have been qualitatively compared.

To compare human and canine routes, only PPH group was used in human group because they are in the same position. The comparisons that have been made between the models depend on the surgical procedures. Thus, for TPA, we decided to compare sagittal (a) and transversal (b) angles. For TAA, (aTAA) mean angle was compared between the 2 models. Student's t-test was applied after confirming normality and homogeneity of variances.

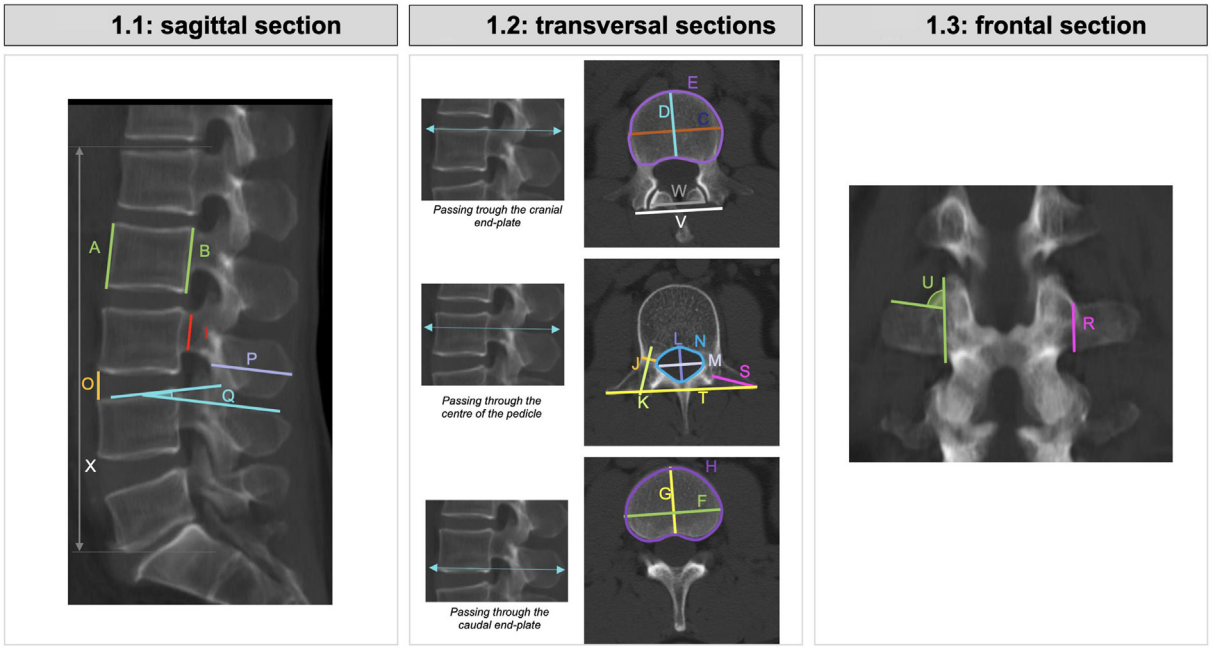

Fig. 1. Measurements from all the bony anatomical vertebral reliefs and IVDs in CT-scan. a) Sagittal view: ventral vertebral body's cranio-caudal distance (A), dorsal vertebral body's cranio-caudal distance (B), pedicle cranio-caudal distance (I), IVD cranio-caudal distance (O), spinous process ventro-dorsal distance (P), spinous process angle (Q) and total lumbar spine length (X). b) Transversal view: cranial end-plate's latero-lateral distance (C), cranial end-plate's ventro-dorsal distance (D), cranial end-plate's area (E), caudal end-plate's latero-lateral distance (F), caudal end-plate's ventro-dorsal distance (G) caudal end-plate's area (H), pedicle latero-medial distance (J) pedicle ventro-dorsal distance (K), vertebral canal ventro-dorsal distance (L), vertebral canal latero-lateral distance(M), vertebral canal area (N), lateral process medio-lateral distance (S) and latero-lateral lateral process total distance (T), cranial articular latero-lateral distance (V) and caudal articular latero-lateral distance (W). c) Frontal view: transverse process cranio-caudal distance (R) and transverse process angle (U).

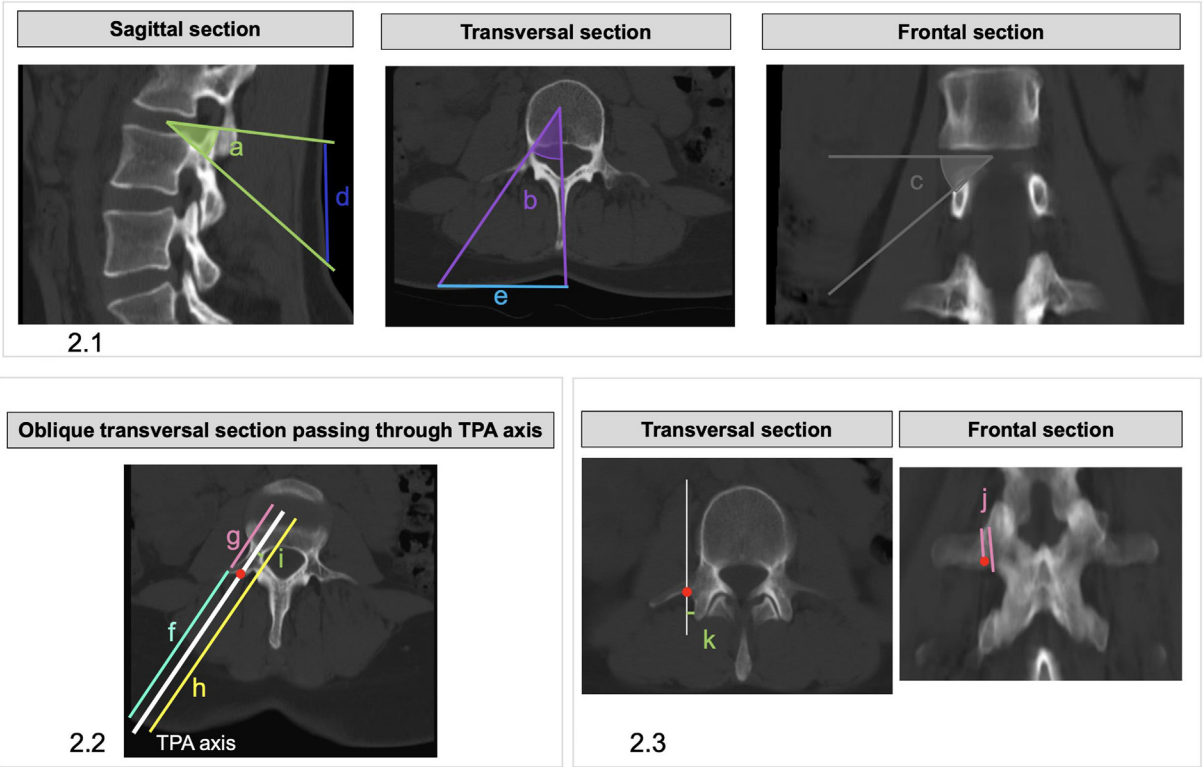

Fig. 2. Measurements of angles and surgical landmarks in a CT-scan for Trans Pedicular Approach (TPA). a) Angle (a): measured in the sagittal plane between the direction of the surgical instrument targeting IVD's center and the transversal plane. Angle (b): measured in the transversal plane between spinous process axis and the sagittal plane. Angle (c): measured in frontal plane between the surgical instrument axis and the transversal plane. (d): cutaneous distance between IVD's transversal plane and cutaneous entry point in sagittal plane. (e): cutaneous distance between spinous process and cutaneous entry point. b) The cross-section is oriented in the needle plane in order to measure the distance between the cutaneous entry point and the bony entry point (f), the distance between the bony entry point and the NP (g). (h): total minimal needle length (h = f + g). (i): minimal distance between the needle way and the spinal canal. c) ratio between the distance "bony entry point-canal edge of the transverse process" and the cranio-caudal total transverse process distance measured in frontal plane (j), distance between the bony entry point and the articular process' lateral edge measured in transversal plane (k).

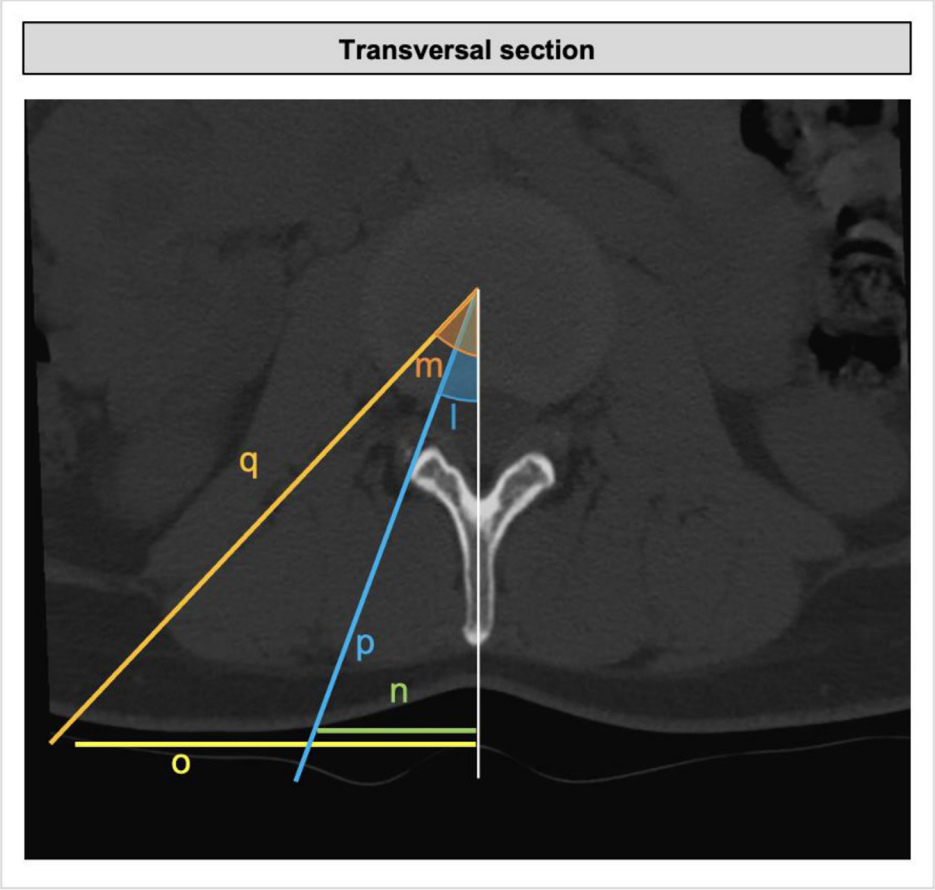

Fig. 3. Measurement of Trans Annular Approach angles in a CT-scan in transversal view. Minimal angle (l) was defined by the intersection between the medial line and the most medial axe of reaching NP by TAA without spinal canal disruption. Maximal angle (m) was defined by the intersection between the medial line and the most lateral axe of reaching NP by TAA avoiding rib and retroperitoneal cavity. Minimal (n) and maximal (o) distances between the medial line and the cutaneous entry point for (l) and (m) were measured. Distances between the cutaneous entry for (l) and (m) angles and NP were measured and noted (p) and (q) respectively.

Table 1
Morphometric measurements (mean and standard deviation SD) in CT scans of human group (H: blue), Labrador/Golden (LG: white) and French Bulldogs (FB: green).

Measure	A(mm)	B(mm)	C(mm)	D(mm)	E(mm²)	F(mm)	G(mm)	H(mm²)	I(mm)	J(mm)	K(mm)	L(mm)
H (mean ± SD)	27.1 ± 2.3	26.5 ± 2.4	48.2 ± 6.2	34.2 ±3.5	1452 ± 292	51.7 ± 5.7	34.5 ± 3.5	1491.5 ± 271	15 ± 2.1	11.7 ± 4.4	27.5 ± 2.8	18.9 ± 3
LG (mean ± SD)	23.1 ± 2.6	25.3 ± 2.5	22.8 ± 2.1	14.1 ± 1.3	303.8 ± 42.5	25.7 ± 2.5	13.4 ± 1.2	311.7 ± 48.8	19.9 ± 2.9	5.3 ± 1.6	20.1 ± 3.6	9.3 ± 1.3
FB (mean ± SD)	14.9 ± 1.8	16.9 ± 2.4	16.4 ± 1.4	9.8 ± 1	156 ± 23.3	19 ± 1.8	9 ± 0.9	159.2 ± 22.8	13.9 ± 1.9	4.3 ± 1	15.2 ± 1.7	7.8 ± 1
Measure	**M(mm)**	**N(mm²)**	**O(mm)**	**P(mm)**	**Q(°)**	**R(mm)**	**S(mm)**	**T(mm)**	**U(°)**	**V(mm)**	**W(mm)**	**X(mm)**
H (mean ± SD)	24.7 ± 2.9	281 ± 70.5	10.5 ± 3.3	35.7 ± 5.5	10.4 ± 3.9	13.9 ± 2.4	25.2 ± 7	88.1 ± 11.5	84.3 ± 8.9	50.8 ± 7.2	40.8 ± 10.1	169.8 ± 14.3
LG (mean ± SD)	12.3 ± 1.2	94.2 ± 17.2	7.1 ± 2.1	30.1 ± 4.2	7.7 ± 5	12.6 ± 2.2	25.7 ± 9.6	64.8 ± 12.1	43.6 ± 10.3	27.6 ± 3.5	18.6 ± 5.7	217.5 ± 13.5
FB (mean ± SD)	9.8 ± 1.1	64.2 ± 11.3	6.1 ± 1.6	21 ± 3.2	8.4 ± 5.1	9 ± 1.5	18 ± 6.6	45.3 ± 9.5	41.9 ± 9.7	20.8 ± 2.1	14.8 ± 3.6	153 ± 29.9

A: ventral vertebral body's cranio-caudal distance. B: dorsal vertebral body's cranio-caudal distance. C: cranial end-plate's latero-lateral distance. D:cranial end-plate's ventro-dorsal. E: cranial end-plate's area. F: caudal end-plate's latero-lateral distance. G: caudal end-plate's ventro-dorsal distance. H: caudal end-plate's area. I:pedicle cranio-caudal distance. J: pedicle latero-medial distance. K: pedicle ventro-dorsal distance. L: vertebral canal ventro-dorsal distance. M: vertebral canal latero-lateral distance. N:vertebral canal area. O: IVD cranio-caudal distance. P: spinous process ventro-dorsal distance. Q: spinous process angle. R: transverse process cranio-caudal distance. S: lateral process medio-lateral distance. T:latero-lateral lateral process total distance. U: transverse process angle. V: cranial articular latero-lateral distance. W: caudal articular latero-lateral distance. X: total lumbar spine length.

3. Results

3.1. Anatomical measurements

CT-scan measurements from all the bony anatomical vertebral reliefs and IVDs are presented in Table 1. Comparing the measures between human and dogs, the cranio-caudal vertebral body distances (A and B) were almost similar between LG group and Human. This measure was 1.8 smaller in FB group compared to Human. In dog group, vertebral bodies were narrower (latero-lateral distance C and F) and less deep (ventro-dorsal distance D and G) than Humans (respectively LG: 22.8 mm ± 2.1, 25.7 mm ± 2.5, 14.1 mm ± 1.3 and 13.4 mm ± 1.2, FB: 16.4 mm ± 1.4, 19 mm ± 1.8, 9.8 mm ± 1 and 9 mm ± 0.9 vs H: 48.2 mm ± 6.2, 51.7 mm ± 5.7, 34.2 mm ± 3.5 and 34.5 mm ± 3.5). Regarding pedicles, cranio-caudal distance (I) was bigger in LG (19.9 mm ± 2.9) compared to Human (15 mm ± 2.1) and almost identically between Human and BF (13.9 mm ± 1.9). Latero-medial distance of pedicles (J) was smaller in dog group (LG: 5.3 mm ± 1.6; FB: 4.3 mm ± 1) compared to Human (11.7 ± 4.4). Additionally, spinal canal (L, M, N) was narrower and spinous process (P) shorter in dogs. Size of transverse process (S and T) was shorter in canine. Finally, size of IVD (O) in dogs appeared thinner (LG: 7.1 mm ± 2.1; FB: 6.1 mm ± 1.6) than Human (10.5 mm ± 3.3). For all measurements in Human and in canine models, no difference was found between males and females.

3.2. Routes' comparison (TPA and TAA)

In all species, regarding the iliac wings volume, lumbo-sacral IVD (L5-S1 or L7-S1 depending on species) was systematically inaccessible by TPA or TAA. Interestingly, contrarily to TPA that need a cranial inclination of the needle, TAA allows to target one supplemental spine level above the lumbo-sacral IVD.

3.2.1. Trans-pedicular approach (TPA)

In Human, sagittal angle (a) was statistically different between Supine Position Human (SPH) group and Prone Position Human (PPH) group (respectively 40.2° ± 7.8 and 36.3° ± 5.8; $p = 0.0006$) (Fig. 4). Transversal angle (b) was different between SPH group and PPH group (respectively 46.8° ± 7.2 and 44.8° ± 5.3; $p < 0.0001$). In canine group, sagittal angle (a) was not statistically different between LG (Labrador and Golden) and FB (French Bulldog) (respectively 45.5° ± 2.7 and 45.5° ± 3.5; $p = 0.96$). Transversal angle (b) was statistically different between LG and FB (respectively 47.5° ± 2.2 and 49.1° ± 3.5; $p < 0.0001$). Statistically differences for the sagittal angle (a) were found when comparing PPH group and canine group with $p < 0.0001$. Additionally, a statistical difference of transversal angle (b) was determined between PPH group and canine group ($p < 0.0001$) (Fig. 4). In the PPH group, the cutaneous distance between the spinous process and the cutaneous entry point was 66 mm ± 21 caudally in the sagittal plane (d) and 79 mm ± 19 laterally in the transversal plane (e). In the PPH group, the mean needle length was 123 mm ± 29 (h) (Table 2). For all measurements in Human and in canine models, no difference was found between males and females.

3.2.2. Trans-annular approach (TAA)

In Human, (aTAA) was 49° (±12.3), 48.9° (±12) and 49.2° (±12) in H, SPH and PPH groups, respectively (Fig. 5). No statistical difference was observed between SPH and PPH groups ($p = 0.77$). In canine group (aTAA) was 67.5° (±24.9), 65.2° (±26.1) and 68.8° (±24.1) for all dogs, LG and FB groups respectively. There was no significant difference between LG and FB ($p = 0.86$). Comparing Human to dogs, there was a significative difference ($p < 0.0001$) between aTAA of PPH group and canine group. In the PPH group, the cutaneous distance between the spinous process and the cutaneous entry point was 79 mm ± 19 laterally for the smaller angle (n) and the mean needle length for this cutaneous

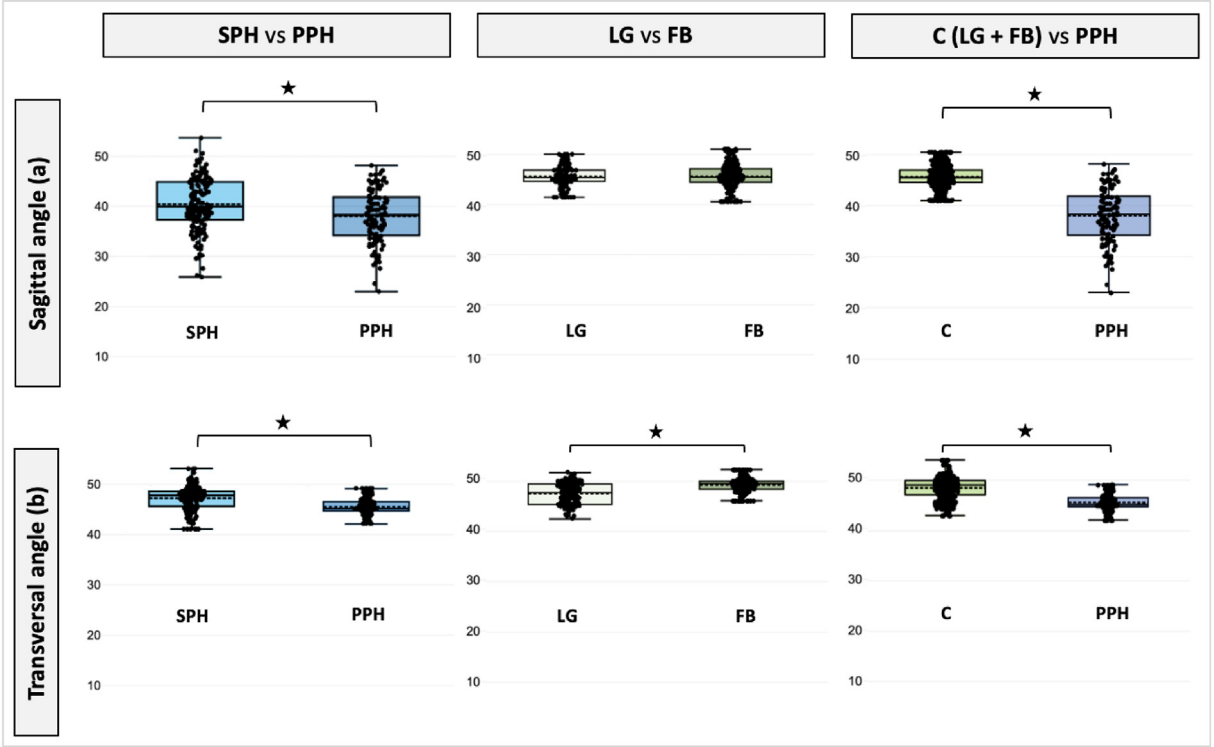

Fig. 4. Comparison of landmark measurement in human and dogs in Trans Pedicular Approach (TPA). The sagittal angle (a) and the transversal angle (b) between SPH (supine position human in light blue) vs PPH (prone position human in dark blue) had significant differences ($p = 0.0006$ and $p < 0.0001$ respectively). The sagittal angle (a) between LG (Labrador and Golden retriever in light green) vs FB (French Bulldog in olive green) had no statistically significant difference ($p = 0.96$). The transversal angle (b) between LG vs FB had a significant difference ($p < 0.0001$). The sagittal angle (a) and transversal angle (b) between C (canine model: LG + BF in green) and PPH had a statistically significant difference ($p < 0.0001$ for both).

Table 2
TPA's measurements (mean and standard deviation SD) for human group (H), supine position human (SPH), prone position human (PPH), canine model (C), Labrador and Golden retriever (LB) and French Bulldog (BF).

Measure	a(°)	b(°)	c(°)	d(mm)	e(mm)	f(mm)	g(mm)	h(mm)	i(mm)	j(mm)	k(mm)
H (mean ± SD)	39.4 ± 5.5	46.5 ± 2.7	37.1 ± 5	73 ± 21.2	83.5 ± 14.8	83.4 ± 21.9	38.7 ± 5.4	122.1 ± 27.3	5.4 ± 1.6	0.9 ± 0.1	2.8 ± 3.6
SPH (mean ± SD)	36.3 ± 5.8	44.8 ± 2.5	35.2 ± 5.3	65.7 ± 20.6	79 ± 15.9	81.2 ± 23.9	41.8 ±5.4	123 ± 29.3	5.1 ± 1.6	0.8 ± 0.2	2.3 ± 2.9
PPH (mean ± SD)	40.2 ± 7.8	46.8 ± 7.2	37.5 ± 7.2	76.3 ± 24.9	87 ± 20	87.3 ± 24.9	36.6 ± 7.1	123.9 ± 32	5.5 ± 1.8	0.9 ± 0.1	2.8 ± 3.4
C (mean ± SD)	45.5 ± 3.2	48.4 ± 2.3	41.8 ± 3.5	47.4 ± 12.3	42.5 ± 10	46.8 ± 16.2	14.8 ± 2.7	61.6 ± 18.9	1.9 ± 0.7	0.5 ± 0.1	2.2 ± 1.5
LG (mean ± SD)	45.5 ± 2.7	47.5 ± 2.2	42.7 ± 3.1	59.3 ± 9.8	52 ± 9.2	57.9 ± 19.7	17 ± 2.1	74.9 ± 21.8	2.4 ± 0.7	0.5 ± 0.1	2.9 ± 1.8
FB (mean ± SD)	45.5 ± 3.5	49.1 ± 2.1	41 ± 3.5	40.3 ± 6.9	36.8 ± 4.9	39.7 ± 7.3	13.2 ± 1.6	52.9 ± 8.9	1.6 ± 0.5	0.5 ± 0.1	1.7 ± 1.1

a angle: angle in the sagittal plane. b angle: angle in the transversal plane. c angle: angle in the frontal plane. d: distance between the IVD's transversal plane and the cutaneous entry point in the sagittal plane. e: distance between the spinous process and the cutaneous entry point in the transversal plane. f: distance between the cutaneous entry point and the bony entry point. g: distance between the bony entry point and the nucleus pulposus. h: the total minimal needle length (h = f + g). i: the minimal distance between the needle way and the spinal canal. j: the ratio between the distance "bony entry point-canal edge of the transverse process" and the cranio-caudal total transverse process distance measured in frontal plane. k: the distance between the bony entry point and the articular process lateral edge measured in transversal plane.

entry point was 111 mm ± 26 laterally (h) (Table 3). For all measurements in Human and in canine model, no difference was found between males and females.

3.2.3. *Intra-rater reliability*

The intra-rater reliability was measured in order to ensure results' quality. Intra-rater reliability revealed very strong agreement (ICC >0.90) for all measures (A: 0.97, B: 0.97, C: 0.99, D: 1, E: 0.999, F: 1, G: 0.99, H: 1, I: 0.99. J: 1, K: 0.93, L: 1, M: 1, N: 1, O: 0.99, P: 0.99, Q: 0.93, R: 0.95. S: 1, T: 1, U: 0.98, V: 1, W: 1).

4. Discussion

This study provides with precise anatomical lumbar spine values for human and 2 canine breeds, one chondrodystrophic and one non-chondrodystrophic (Golden/Labrador Retriever and French Bulldogs). This database will assist future researchers in creating comparisons between the human and canine models, as the dog is becoming a recognized model for disc degeneration. Human surgeons will have access to numerical data that will allow them to safely translate well-established human surgical procedures to a model with which they are less familiar, to develop new regenerative therapy approaches. While measurements of human spine anatomy are in accordance with the literature [12,13], it is the first time, to our knowledge, that they are characterized for a non-chondrodystrophic medium-sized breed (Golden/Labrador Retriever) and a chondrodystrophic brachymorphic breed (French Bulldogs). Moreover, this study expands IVD routes guideline for human and canine models. Historically, IVD percutaneous approaches were used to perform discography replaced now by non-invasive explorations. Recently, in the context of IVD regenerative medicine based on the

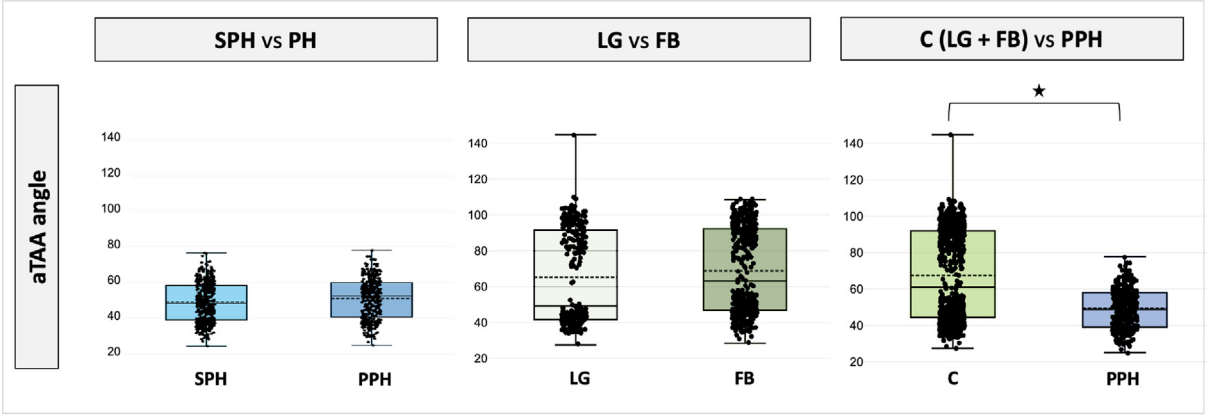

Fig. 5. Comparison of landmark measurement in human and dogs in Trans Annular Approach (TAA). In Trans Annular Approach (TAA) there is no significant differences for (aTAA) angle between SPH (supine position human in light blue) vs PPH (prone position human in dark blue) ($p = 0.77$) nor between LG (Labrador and Golden retriever in light green) versus FB (French Bulldog in olive green) ($p = 0.86$). Nevertheless, there was a significant difference between PPH vs C (canine model: LG + FB in green) ($p < 0.001$).

Table 3
TAA's measurements (mean and standard deviation SD) for human group (H), supine position human (SPH), prone position human (PPH), canine model (C), Labrador and Golden retriever (LB) and French Bulldog (BF).

	l (°)	m(°)	aTAA(°)	n(mm)	o(mm)	p(mm)	q(mm)
H (mean ± SD)	40.1 ± 7.3	58 ± 8.8	49 ± 12.3	71.6 ± 20.4	111.4 ± 26	110.1 ± 21.9	130.2 ± 24.4
PPH (mean ± SD)	38.8 ± 10	58.2 ± 13.4	49.2 ± 12.7	69.7 ± 23	114.1 ± 29.6	110.8 ± 26.3	132.7 ± 29.9
SPH (mean ± SD)	40.1 ± 7.3	57.8 ± 8.9	48.9 ± 12	72.1 ± 20.9	110.8 ± 27.6	110.9 ± 23.9	130.9 ± 26.5
C (mean ± SD)	44.5 ± 6.8	90.4 ± 12	67.5 ± 24.9	37.8 ± 8.4	87.1 ± 18.7	52 ± 11	72.7 ± 14.4
LG (mean ± SD)	40.9 ± 4.1	89.5 ± 12.6	65.2 ± 26.1	43.8 ± 7.3	104.9 ± 16.2	63.3 ± 8.7	87 ± 11.5
FB (mean ± SD)	46.6 ± 7.2	91 ± 11.7	68.8 ± 24.1	34.9 ± 7.2	78.1 ± 11.9	46.4 ± 6.8	65.4 ± 9

l: minimal angle between the medial line and the most medial axe of reaching the nucleus pulposus (NP) without spinal canal disruption. m: maximal angle between the medial line and the most lateral axe of reaching the NP avoiding rib and retroperitoneal cavity. aTAA angle: mean between l and m angles. n: distance between the medial line and the cutaneous entry point for l angle. o: distance between the medial line and the cutaneous entry point for m angle. p: distance between the cutaneous entry point for l angle and the NP. q: distance between the cutaneous entry point for m angle and the NP.

injection of cells, biological factors or biomaterials into the NP, minimally invasive IVD approaches arouse interest. The current "gold standard" for targeting the NP is the percutaneous dorsolateral route involving needle puncture of the *annulus fibrosus* (AF) (TAA's equivalent) [5]. However, it is now well recognized that the TAA can lead to in-depth alteration of the mechanical properties of the AF. Such AF impairments are known to lead to an increased risk of NP herniation and accelerated IVD degeneration, as demonstrated in animal models [14] and in human studies [15].

TPA was described by Vadalà et *al.* in human and ovine models [6,16] and considered as an alternative. Nevertheless, TPA exhibits significant risks of secondary lesions: spinal canal disruption with possible neurological consequences, vertebral endplate's fracture and end-plate healing defects [17]. Vertebral canal disruption risk increases when the size of

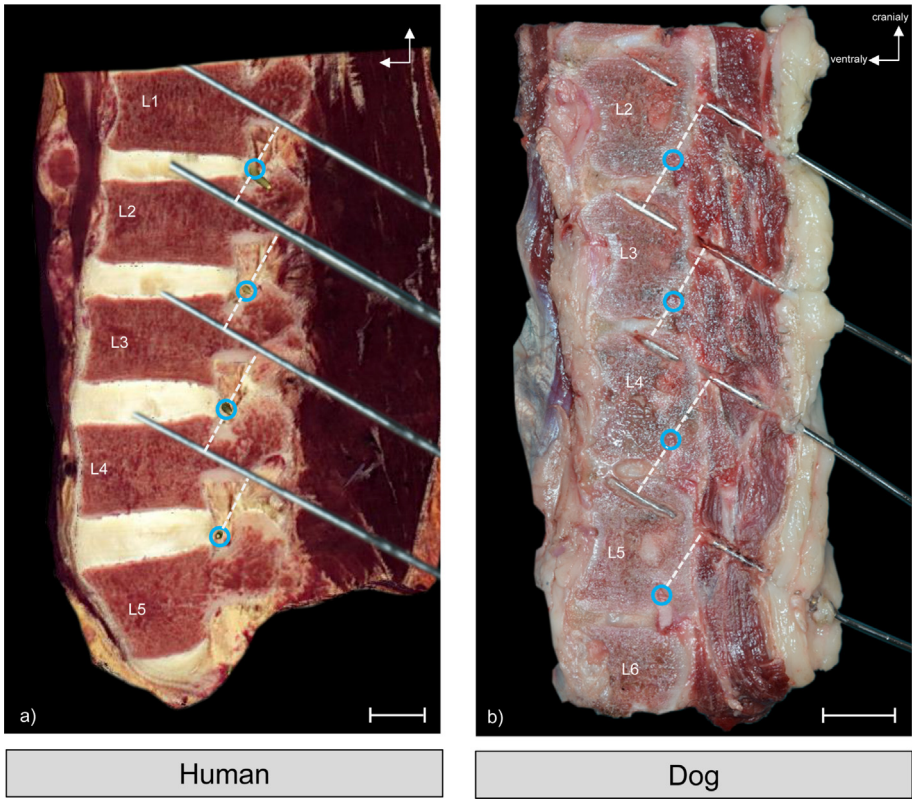

Fig. 6. Lumbar spine anatomical sagittal sections of a human (a) and a dog (b) in a plane of TPA routes. For the dog spine, 4 TPA were performed *ex vivo* with a Kirschner wire under radioscopy using angles (a), (b) and (c) previously established. Spines were then removed, frozen and sections were performed in the plane of the wires. For the human spine, a section in the theoretical sagittal plan of the TPA was made by a virtual dissection table (Anatomage® Table 7.0 – Milan). The distances between the Kirschner wires and the adjacent nerve roots were measured. Adjacent nerve roots (blue circle) were at distant from TPA (dog: 14.3 mm, human: 19 mm). Scale bar: 20 mm.

the animal model decrease. Vadalà et al. suggest angles of 49.6° in the sagittal plane and 47.5° in the frontal plane to target the NP through caudal vertebra [6] regardless of model (ovine and human). In our study, a higher number of measurements on a significant number of IVDs have been defined and demonstrated TPA's orientations were not the same between species (example for TPA's sagittal (a) angle: 36.3° for Humans and 45.5° for dogs). These differences could be explained by the patient's position on the operating table as demonstrated in this study (significant difference between the TPA's sagittal angle (a) in supine position (40.2°) and in prone position (36.3°)). Thus, preoperative planning by imaging in prone position would avoid as much as possible vertebral canal disruption. Furthermore, nerve roots must be considered. TPA routes were widely distant from adjacent nerve roots, as we have shown in anatomical sections of a human and a dog (respectively: 19 mm and 14.3 mm) (Fig. 6). Concerning TAA, Kambin's triangle [18] must be considered and the minimal TAA angle shall be chosen to avoid nerve root injury. Technically, choosing the minimal TAA angle correspond to the shortest needle with a smallest dead volume and facilitate NP injection.

The TAA is controversial regarding AF lesions [14,15]. O'Connell et al. have shown that the risk of DDD induction after AF lesion post-injection is not constant, as it depends on the ratio between the diameter of the needle and the height of the IVD [19]. According to Elliott et al., when the gauge of the needle is less than 40 % of the height of the IVD, AF puncture does not induce accelerated DDD [20]. This precaution seems easy to implement and should be systematic in clinical practice.

These two IVD approaches appear feasible, according to relevant CT-scan measurements. It is well known that angles measurements may change slightly (e.g. 5 % variation for Cobb's angle) without major clinical consequences or implications [21]. The same is true when significant differences in angles between models are observed. However, this study showed angles measured in TPA have small standard deviations, indicating it is necessary to be accurate in order to perform TPA. It was not true for TAA: to perform a safety approach, the angle of the needle can be within a minimal angle (l) and maximal angle (m). Thus, performing TPA required more precision than TAA, regardless of the model used.

This study provides lots of accurate landmarks and will guide surgeons, radiologists, veterinarian in their reflection before performing IVD approaches for DDD depending on the species treated. For example, when considering TPA canine models allow a greater margin of error in the sagittal plane (greater cranio-caudal pedicle distance), but carries a greater risk of spinal canal disruption (reduced latero-medial pedicle distance) [17]. In DDD research, chondrodystrophic dogs (French Bulldogs) constitute a relevant veterinary model as they exhibit early DDD. Non chondrodystrophic dogs (Golden/Labrador Retriever) could be the control group.

5. Conclusion and perspectives

This study develops a solid database of morphometric lumbar spine characteristics in human and canine models. By detailing anatomical landmarks and ensuring precision in percutaneous IVD's injection procedures in human and canine models, the study provides surgeons and researchers with the necessary data in human and canine models to access the IVD safely within the context of translational protocols from preclinical in canine models to clinical human studies.

Author contributions

Conception and design: N. Gavira, C. Decante, J. Guicheux, J. Clouet, and M. Fusellier.

Analysis and interpretation of the data: N. Gavira, C. Decante, N. Bouhsina1 B. Miannay, M. Fusellier.

Drafting of the article: N. Gavira, C. Decante, J. Clouet, and M. Fusellier.

Critical revision of the article for important intellectual content: N. Gavira, C. Decante, N. Bouhsina, D. Rouleau, B. Miannay, N. Bronsard, A. David, R. Jossier, J. Guicheux, J. Clouet, and M. Fusellier.

Final approval of the article: N. Gavira, C. Decante, N. Bouhsina, D. Rouleau, B. Miannay, N. Bronsard, A. David, R. Jossier, J. Guicheux, J. Clouet, and M. Fusellier.

Provision of study materials or patients: N. Gavira, N. Bouhsina, D. Rouleau, B. Miannay, N. Bronsard, A. David, R. Jossier, M. Fusellier.

Statistical expertise: N. Gavira, C. Decante, B. Miannay.

Obtaining of funding: J. Guicheux, J. Clouet, and M. Fusellier.

Administrative, technical, or logistic support: D. Rouleau, B. Miannay, A. David, M. Fusellier.

Collection and assembly of data: N. Gavira, C. Decante, N. Bouhsina, D. Rouleau, B. Miannay, N. Bronsard, A. David, R. Jossier, M. Fusellier.

Ethics approval

All applicable international, national, and/or institutional guidelines for the care and use of animals were adhered to. All procedures involving animals performed in this study were in accordance with the ‘‘3Rs’’ rule (Replacement, Reduction, and Refinement), the ethics standards of the institution and the practice at which the study was performed. This study was approved by the French Ministry of Agriculture, by the ethics committee of the Pays de la Loire Region (Ethics approval number APAFIS: 8401) and by the Centre of Research and Pre-clinical Investigations (CRIP) at the ONIRIS-National Veterinary School of Nantes. This study was also performed in accordance with the ethical standards as laid down in the 1964 Declaration of Helsinki and its later amendments or comparable ethical standards. the study is reported in accordance with ARRIVE guidelines.

For experiments involving human participants, informed consents have been obtained from all subjects and/or their legal guardian(s). All the human tissues used come from cadaveric anatomical specimen donated to Research, the consents having been obtained during their lifetime. Local Institutional Review Board and Ethics Committee approval was obtained for the use of human anatomical specimens.

Declaration of Generative AI and AI-assisted technologies in the writing process

All of the authors declare that they didn't use AI and AI-assisted technologies in the writing process.

Funding sources

This study was supported by grants from the Société Française de Chirurgie du Rachis, the Institut National de la Santé et de la Recherche Médicale (INSERM), the Région des Pays de la Loire and RFI BIOREGATE (DISCODOG Project) and Agence Nationale de la Recherche ANR-16-CE18-0008-01. The sponsors had no involvement in the design, collection, analysis and interpretation of data; in the writing of the manuscript and in the decision to submit the manuscript for publication.

Declaration of competing interest

All of the authors declare that they have no potential conflicts of interests.

Acknowledgments

The authors gratefully acknowledge the technical assistance that they received from the personnel of the CRIP (Centre de Recherche et d’Investigation Pré-clinique, i.e., Patrice Roy, Stéphane Madec and Ingrid Leborgne), from Stéphane Lagier and Yvan Blin (Laboratoire d’Anatomie, Faculté de Médecine, Nantes) and Sophie Domingues (Longdom publishing) for editing the manuscript.

References

[1] Z.I. Johnson, Z.R. Schoepflin, H. Choi, I.M. Shapiro, M.V. Risbud, Disc in flames : roles of TNF- α and IL-1 β in intervertebral disc degeneration, Eur. Cell. Mater. 30 (2015) 104–117.

[2] J.N. Katz, Lumbar disc disorders and low-back pain: socioeconomic factors and consequences, J Bone Jt Surg. 88 (Suppl 2) (2006 Apr) 21–24.

[3] N. Henry, P. Colombier, L. Lescaudron, O. Hamel, J. Le Bideau, J. Guicheux, et al., Regenerative Medicine of the Intervertebral Disc: from Pathophysiology to Clinical Application, vol. 30, Medicine/Sciences, 2014, pp. 1091–1100.

[4] J. Clouet, M. Fusellier, A. Camus, C. Le Visage, J. Guicheux, Intervertebral disc regeneration: from cell therapy to the development of novel bioinspired endogenous repair strategies, Adv. Drug Deliv. Rev. 146 (2019) 306–324.

[5] L. Kapural, A. Goyle, Imaging for provocative discography and minimally invasive percutaneous procedures for treatment of discogenic lower back pain, Tech. Reg. Anesth. Pain Manag. 11 (2) (2007 Apr) 73–80.

[6] G. Vadalà, F. De Strobel, M. Bernardini, L. Denaro, D. D'Avella, V. Denaro, The transpedicular approach for the study of intervertebral disc regeneration strategies: in vivo characterization, Eur. Spine J. 22 (Suppl 6) (2013 Nov) S972–S978.

[7] L. Le Fournier, M. Fusellier, B. Halgand, J. Lesoeur, O. Gauthier, P. Menei, et al., The transpedicular surgical approach for the development of intervertebral disc targeting regenerative strategies in an ovine model, Eur. Spine J. 26 (8) (2017) 2072–2083.

[8] M. Alini, S.M. Eisenstein, K. Ito, C. Little, A. Kettler, K. Masuda, et al., Are animal models useful for studying human disc disorders/degeneration? Eur. Spine J. 17 (1) (2008) 2–19.

[9] M. Fusellier, J. Clouet, O. Gauthier, M. Tryfonidou, C. Le Visage, J. Guicheux, Degenerative lumbar disc disease: in vivo data support the rationale for the selection of appropriate animal models, Eur. Cell. Mater. 39 (2020) 18–47.

[10] N. Bergknut, J.P.H.J. Rutges, H.-J.C. Kranenburg, L. Smolders, R. Hagman, H.-J. Smidt, et al., The dog as an animal model for intervertebral disc degeneration? Spine 37 (5) (2012) 351–358.

[11] N.N. Lee, J.S. Kramer, A.M. Stoker, C.C. Bozynski, C.R. Cook, J.T. Stannard, et al., Canine models of spine disorders, JOR Spine 3 (4) (2020) 1–20.

[12] S.R. Sheng, X.Y. Wang, H.Z. Xu, G.Q. Zhu, Y.F. Zhou, Anatomy of large animal spines and its comparison to the human spine: a systematic review, Eur. Spine J. 19 (1) (2010) 46–56.

[13] B.L. Showalter, J.C. Beckstein, J.T. Martin, E. Elizabeth, A.A.E. Orías, T.P. Schaer, et al., Comparison of animal discs used in disc research to human lumbar disc : torsion mechanics and collagen content, Spine 37 (15) (2013) 1–17.

[14] S. Sobajima, J.F. Kompel, J.S. Kim, C.J. Wallach, D.D. Robertson, M.T. Vogt, et al., A slowly progressive and reproducible animal model of intervertebral disc degeneration characterized by MRI, X-ray, and histology, Spine 30 (1) (2005) 15–24.

[15] E.J. Carragee, A.S. Don, E.L. Hurwitz, J.M. Cuéllar, J.A. Carrino, J. Carrino, et al., 2009 ISSLS Prize Winner: does discography cause accelerated progression of degeneration changes in the lumbar disc: a ten-year matched cohort study, Spine 34 (21) (2009) 2338–2345.

[16] G. Vadalà, F. Russo, G. Pattappa, D. Schiuma, M. Peroglio, L.M. Benneker, al er, The transpedicular approach as an alternative route for intervertebral disc regeneration, Spine 38 (6) (2013) 319–324.

[17] C. Decante, J. Clouet, A. Hamel, L. Le Fournier, O. Gauthier, D. Rouleau, et al., Collateral effects of targeting the nucleus pulposus via a transpedicular or transannular surgical route: a combined X-ray, MRI, and histological long-term descriptive study in sheep, Eur. Spine J. 30 (2) (2020 Feb) 585–595.

[18] P. Kambin, M.D. Brager, Percutaneous posterolateral discectomy. Anatomy and mechanism, Clin. Orthop. Relat. Res. 223 (1987 Oct) 145–154.

[19] G.D. O'Connell, E.J. Vresilovic, D.M. Elliott, Comparison of animals used in disc research to human lumbar disc geometry, Spine 32 (3) (2007) 328–333.

[20] D.M. Elliott, C.S. Yerramalli, J.C. Beckstein, J.I. Boxberger, W. Johannessen, E.J. Vresilovic, The effect of relative needle diameter in puncture and sham injection animal models of degeneration, Spine 33 (6) (2008) 588–596.

[21] D.L. Carman, R.H. Browne, J.G. Birch, Measurement of scoliosis and kyphosis radiographs. Intraobserver and interobserver variation, J Bone Joint Surg Am 72 (3) (1990 Mar) 328–333.